ENHANCEMENT OF HEAT TRANSFER IN A PLATE HEAT EXCHANGER BY TURBULENCE PROMOTORS

R. Tauscher, F. Mayinger
Lehrstuhl A für Thermodynamik
Technische Universität München
Arcisstr. 21, 80333 München
Phone number: + + 49 89-289 16 221, Fax number: + + 49 89-289 16 218
E-mail: tauscher@thermo-a.mw.tu-muenchen.de

ABSTRACT: The paper presents an experimental and numerical investigation of the forced convective heat transfer in flat channels with rectangular cross section. To enhance the heat transfer, rib-roughened surfaces are applied to the wider walls of the duct. Various rib shapes, rib spacings and rib arrangements have been investigated. Temperature fields and velocity fields in the heat exchanger channel were obtained by holographic interferometry and laser-doppler-anemometry, enabling measurements of the thermohydraulic behavior of the flow without disturbing the flow pattern in the channel. By measuring the mean fluid temperatures at the entrance and the exit of the test section as well as the pressure drop, the mean heat transfer and the heat exchanger performance could be judged. Simultaneously with the experimental investigations numerical calculations with a commercial code (TASCflow3D) have been performed.

1. INTRODUCTION

Compact heat exchangers are key components in the development of future air- and spacecraft. The enhancement of heat transfer results in smaller size and weight of the heat exchangers or allows a higher thermal load. The high surface area densities of compact heat exchangers lead to ducts with small aspect ratios. To avoid high pressure drop and pumping power for the fluid, low velocity flow is often applied. The investigations described in this paper have the goal to increase the efficiency of the heat exchangers by the optimization of heat transfer at equal pumping power. Thermohydraulic behavior of an air flow (Pr = 0.7) at Reynolds numbers within a range from Re = 250 to 7000 in a rectangular, isothermically heated duct was investigated. Variations of parameters like rib shape, size, arrangement and duct height were performed. The investigations concentrated on the measurement of global and local heat transfer, pressure drop, velocity fields and turbulence fields. Also, numerical calculations were carried out, mainly to verify the commercial code used (TASCflow3D), but also to allow the investigation of further parameter variations by computer only. Numerous investigations exist on heat transfer and pressure drop in rib-roughened channels. An overview is given by Bergles [Bergles, 1995, 1996] Some pertinent references are given as follows: The effect of transverse vortex generators on heat transfer and pressure drop was examined for Reynolds numbers up to

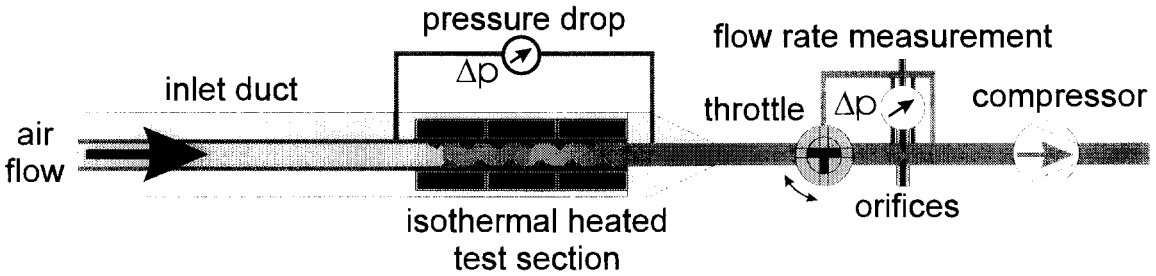

Figure 1. Experimental apparatus

Re=2,000. [Fiebig, 1996] Han performed experiments to investigate the effects of rib-angle-of-attack and channel aspect ratios in short rectangular channels (Re=10,000-60,000). [Han, 1984] Kreipe made investigations on heat transfer and pressure drop in tubes with artificial roughness. [Kreipe, 1985] The influence of circular ribs in flat-oval channels was described by Rifert (Re=4,500-40,000). [Riefert, 1996] Zukauskas presents investigations on the influence of rib shape on global heat transfer and pressure drop for Reynolds numbers Re=6,000-100,000. [Zukauskas, 1989]

2. EXPERIMENT

2.1 Experimental Setup

A schematic of the experimental apparatus is shown in figure 1. Ambient air is sucked into the inlet section of the heat exchanger by a compressor equipped with a flow-regulating throttle. The unheated inlet section leads to an almost hydrodynamically developed flow, with a thermally developing flow regime in the heated test section. The test section (figure 2) consists of a rectangular duct (length L = 300 mm, width W = 150 mm, height H = 10 and 14 mm) with isothermically heated (T_W=50°C) upper and lower aluminium walls. The side walls are made of glass to allow optical access. The test section is connected to a smooth 700 mm inlet duct (adiabatic) and a 150 mm outlet duct with the same aspect ratio. The upper and lower test-section walls have rib-roughened surfaces. Volume flow rates in the channel are determined by the pressure drop at orifices, and verified by rotameters. Air temperatures at the entrance and at the exit of the test section are measured by thermocouples. Pressure drop in the test section is measured by an inclined tube manometer. The mean heat transfer rate in the duct was calculated from temperature and flow rate measurements of the air flow.

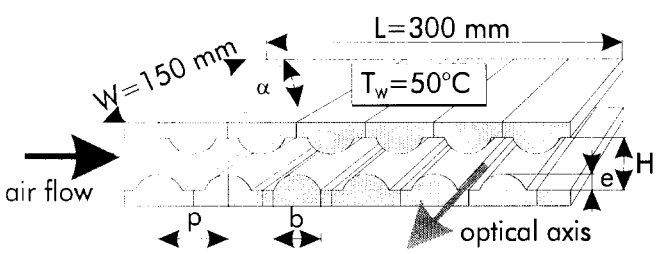

Figure 2. Test section

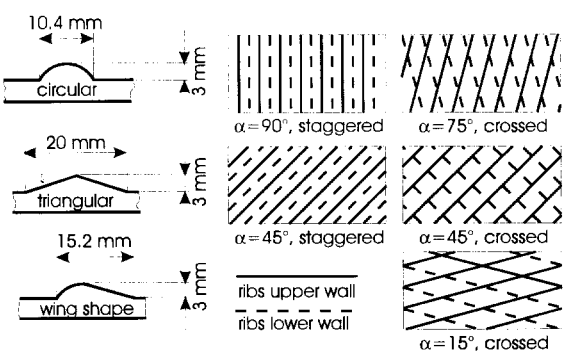

Figure 3. Rib shape and rib arrangement

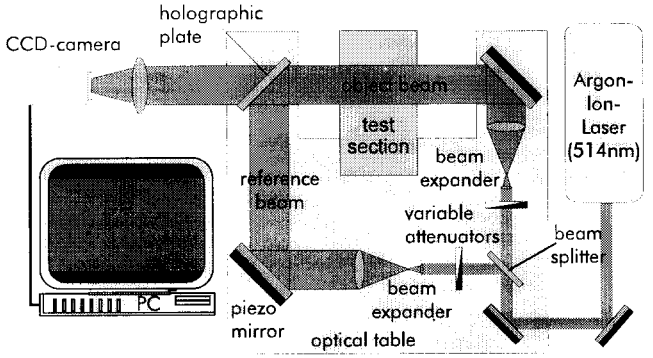

Figure 4. Setup for holographic interferometry (real time method)

2.2 Variation of parameters

The following arrangements have been investigated experimentally (figure 3):

- smooth channel / rib roughened surface
- rib shape (circular, triangular, wing shaped)
- rib spacing: p/e = 6.67, 10, 13.3, 15, 16.67, 20, 20.67
- rib angle and arrangement: α = 15° crossed, α = 45° crossed, α = 75° crossed, α = 45° staggered, α = 90° staggered

2.3 Setup for optical measurements

Two-dimensional temperature fields, and thus the local heat transfer in the duct, were obtained by holographic interferometry measurements. The experimental setup for the holographic interferometry (real-time method) is illustrated in figure 4. This optical measurement technique allows the continuous visualization the two-dimensional temperature field in the duct flow, avoiding any influence on the effect to be measured and shows the thermohydraulic flow pattern in the duct in real time. Detailed explanation of this measurement technique are given by Hauf and Mayinger. [Hauf, 1970, Mayinger, 1974, 1985] For the understanding of the interferograms shown in this paper (figure 6) it is only important to mention that the interference lines (black and white fringes) of the interferograms are approximatively equal to the isotherms of the investigated two dimensional flow. From the distance between these isotherms, the temperature gradient and, therefore, the local heat flux, the local heat transfer coefficient and the local Nusselt number can be calculated. A digital-image-processing system was used for the evaluation of the interferograms. Velocity profiles and kinetic energy of turbulence were determined by LDV-measurements in the free cross section area as well as in the recirculating zones.

3. RESULTS

In order to obtain reference measurements, a smooth channel was investigated first (the data for which were compared to that of other authors, figure 5), and then the channel with various rib-roughened wall configurations was tested (calorimetric measurements). [Gröber, 1955] The second verification of the measurement techniques was the comparison of the integrated local heat transfer (holographic measurements) and the mean global heat transfer (calorimetric measurements). With differences of of less then 5 % in the measured heat transfer rate over the whole Reynolds number range the reliability of the measurement techniques could be confirmed. Figure 6 shows interferograms of the duct flow at different Reynolds numbers (500, 1500, 2500 and 5000) for the rib spacings p/e=10 and p/e=20; the fringes represent isothermal lines in the temperature field.

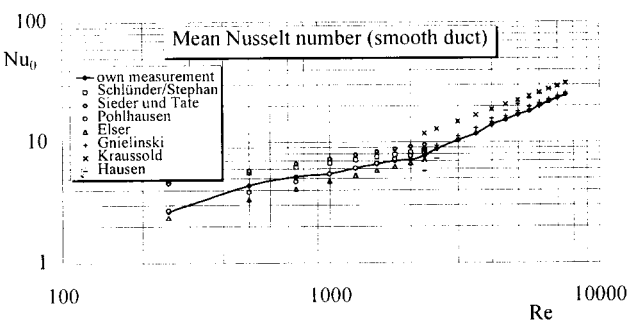

Figure 5. Verification of calorimetric measurements

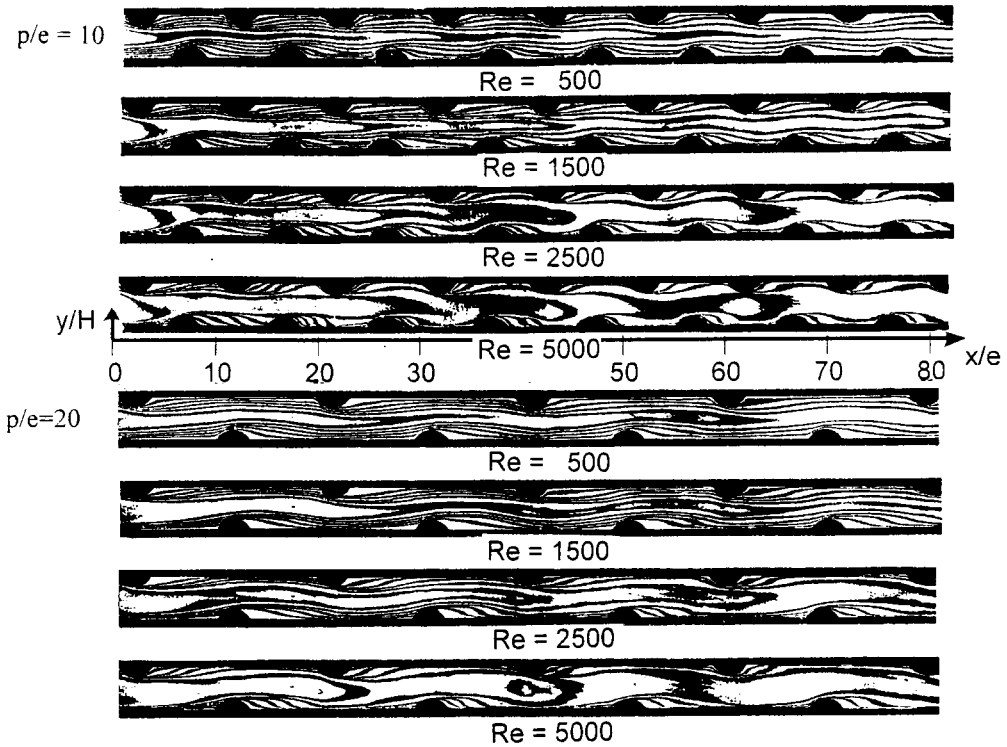

Figure 6. Interferograms of duct flow at Re = 500, 1500, 2500 and 5000, p/e = 10 and p/e=20

These interferograms show the size of the recirculation zones behind the ribs and the wall reattachment point of the flow. The effect of the ribs to induce turbulence can be seen especially in the interferograms for Re=1500. While the flow is still laminar at the beginning of the test section, it becomes turbulent approximately in the middle and is fully turbulent at the end. Out of these interferograms, the local heat transfer can be calculated (figure 7) by measuring the distances of the isotherms along perpendicular lines to the heat transfering surface. [Mayinger, 1993] It can be

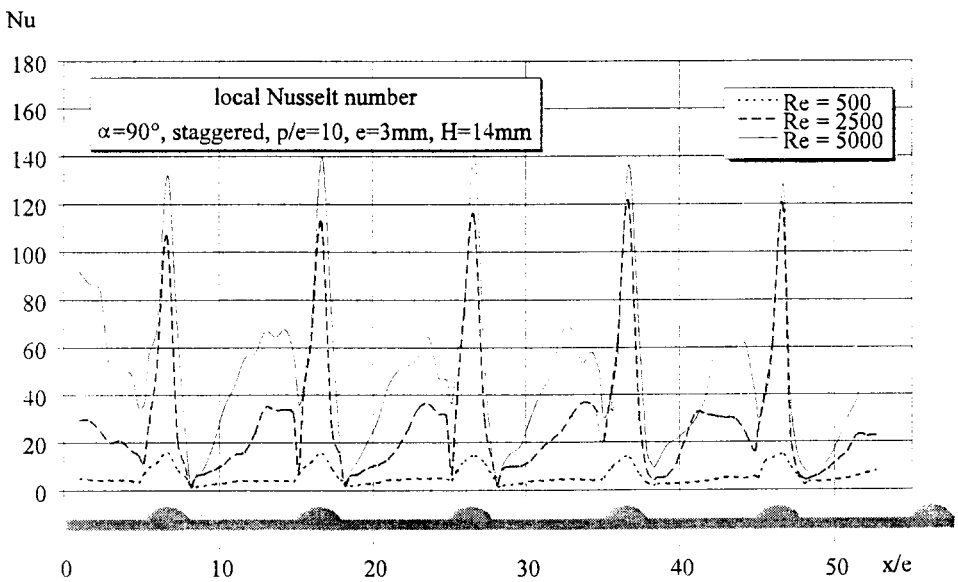

Figure 7. Local Nusselt number in heat exchanger channel with transverse ribs

seen that the Nusselt number always has a maximum located almost at the top of a rib, a minimum just behind the ribs, and, depending on Reynolds number, a second local maximum in the spacing between the ribs. This is due to the fact that at a certain velocity, the flow separates at the rib top, and areas behind the ribs develop where the fluid is recirculating, causing poor heat transfer in this area. The local maxima in the Nusselt number in the spaces between the ribs result from reattaching flow. Higher flow velocities lead to an increase in the mean heat transfer. Figure 7 confirms that the increase results mainly from a better heat transfer between the ribs, while the heat transfer at the ribs itselfs increases only slightly. The turbulence-inducing effect of the ribs can also be determined by LDV measurements of the turbulence intensity of the flow (figure 8). This figure also shows velocity profiles in the duct, and confirms the recirculation zones by showing the negative velocities. Please note the various scaling at the velocity profiles at different Reynolds numbers.

There exist numerous ways to describe the performance of a heat transferring system. One criterion to judge the performance of a configuration is to evaluate the increase in Nusselt number of the rib-roughened channel compared to a smooth channel (Nu/Nu_0) in relation to the ratio of friction factor between a rough and a smooth channel $(\xi/\xi_0)^{1/3}$, which is used in this paper. By means of this kind of comparison, all the data refer to the same pumping power for the fluid $(Nu/Nu_0)/(\xi/\xi_0)^{1/3}$ vs. Re).

In Figure 9 calorimetric measurements are presented to show the influence of rib spacing on heat transfer and friction factor. To judge the performance of the different configurations we

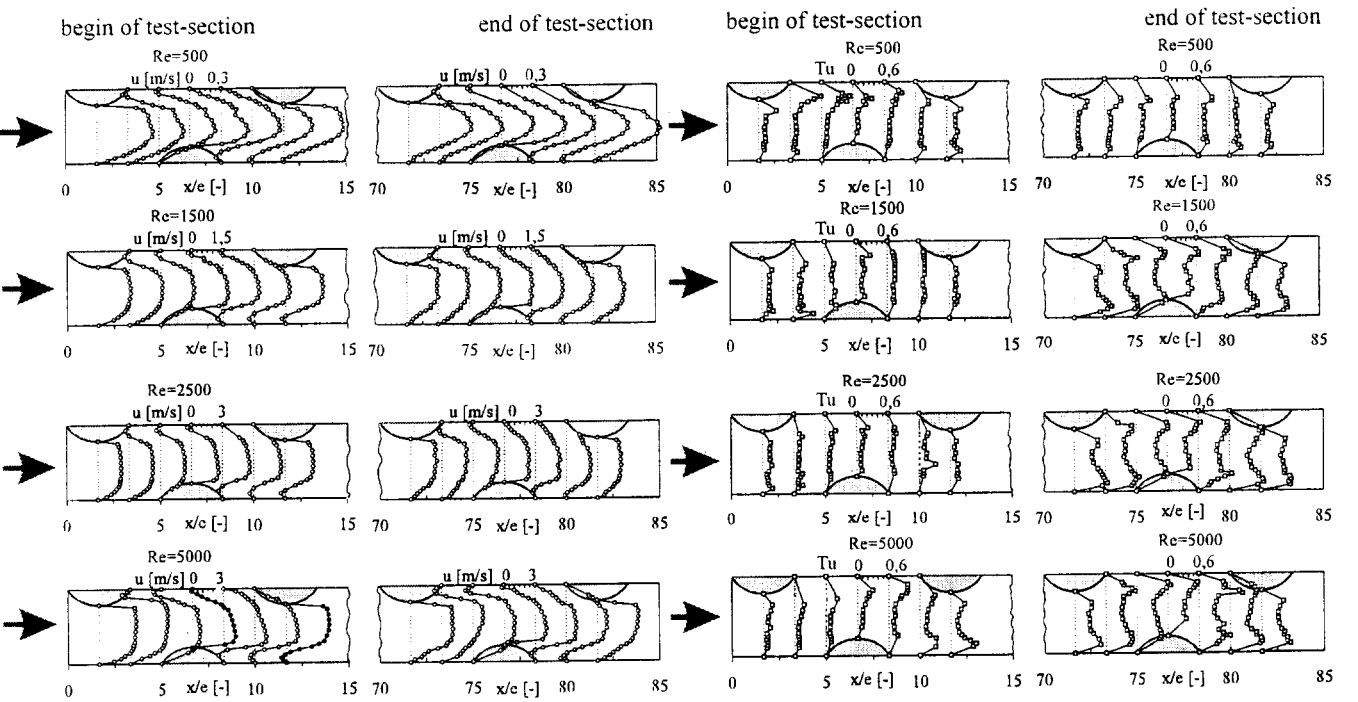

Figure 8. Velocity profiles and turbulence intensity on vertical lines (α=90°, p/e=10, staggered)

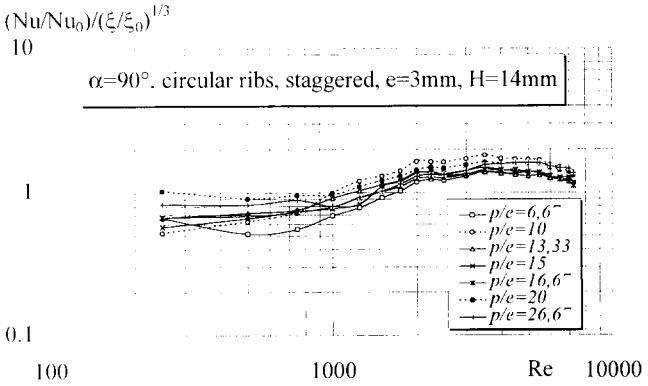

Figure 9. Influence of rib spacing p/e on heat exchanger performance

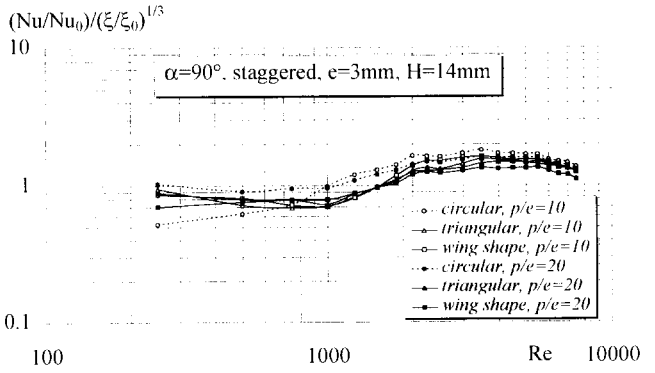

Figure 10. Influence of rib shape on heat exchanger performance

have to examine the laminar and the turbulent region separately. In laminar flow the larger spacings show a better performance than the smaller spacings, due to their comparatively low pressure drop. But nevertheless the performance is worse for all spacings compared to a smooth channel. In the transition region, where the ribs can induce turbulence the performance of the ribbed surfaces gets better. It can be seen that a spacing of p/e = 10 works best for turbulent flow when one considers both heat transfer and friction factor. The diagram also shows the start of the transition from laminar to turbulent flow, depending on Reynolds number and rib spacing.

The influence of rib shape on heat transfer is depicted in Figure 10. One can see that the circular ribs show the best results at all velocities, followed by the wing-shaped ribs. Both diagrams show that turbulence promotors in laminar flow lead to a worse heat transfer at equal pumping power compared to a smooth duct. As noted in Figure 3 and Figure 8, the ribs cannot induce turbulence up to a Reynolds number of Re < 1000 because of the viscous damping effect of the fluid. As soon as the ribs can induce turbulent flow, the performance of the rib roughened channels increases, and almost a two times better performance can be achieved.

Further parameters which infiuence the flow behavior strongly are the rib angle of inclination versus main flow direction and the rib arrangement (crossed, staggered) (figure 11). Considering both heat transfer and pressure drop, the performance of the crossed arrangements will get better the more the rib angle increases. But in any case a rib angle of 45° for the parallel, staggered arrangement shows the best performance over the whole Reynolds number range. The heat transfer rate at equal pumping power can reach about 2.3 times better values than a smooth channel.

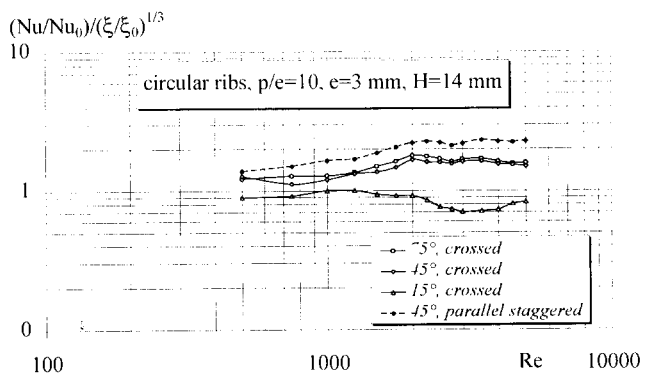

Figure 11. Influence of rib angle α and arrangement on heat exchanger performance

4. NUMERICAL CALCULATIONS

The numerical simulation of the fluid flow in the heat exchanger channel with rib-roughened surfaces was done with the commercial code TASCflow3D. This code works with a finite volume method based on finite elements. The advantage of the finite volume method lies in the inherent conservatism, i.e. the conservation equations are fulfilled automatically. Influences of turbulence are considered with the k-ε model. The boundary layer close to the walls is taken into account by particular wall functions, assuming a logarithmic velocity profile. This ensures the fulfillment of the zero slip condition at the wall on the one hand; on the other hand, the influence of friction is considered without the need to resolve this area with a very dense grid. The boundary conditions and the geometry were modelled exactly as in the experimental setup. Due to the rib angle of $\alpha = 90°$ a two-dimensional flow can be assumed, and thus a reduction of computational grid nodes is achieved to reduce CPU time.

In Figure 12 and 13 the experimental results are compared to numerical calculations with the code TASCflow3D (pressure drop and Nusselt number). The numerical calculations show good agreement with the experimental results in laminar and low turbulent flow. While the calculated pressure drop is higher than the measured one, the calculated heat transfer in turbulent flow is less then in the experiments. The difference between the predictions and experimental results (for heat transfer) increases in the transition region and at higher Reynolds numbers, apparently due to the turbulence model (standard k-ε model) used by the code. In future calculations, three-dimensional arrangements, as well as higher Reynolds number flow, will be investigated numerically, and different turbulence models of new code releases will be tested.

5. CONCLUDING REMARKS

Ribs applied to the heat transfering surfaces of the heat exchanger ducts can induce turbulence and cause an earlier transition from laminar to turbulent flow compared to a smooth duct. Using circular ribs with a spacing of p/e=10, the heat transfer at equal pumping power can almost be doubled in turbulent flow (Re > 2000). Further improvements can be reached by a variation of the rib angle of attack.

Although numerical simulation shows not so bad results, there is still need of improvement of the commercial codes, considering especially turbulence models for the transition region.

Future investigations will also concentrate on channels without an inlet calming length as well as on ducts with smaller rectangular passages to get results for geometries which are closer to heat exchangers commonly found in practice.

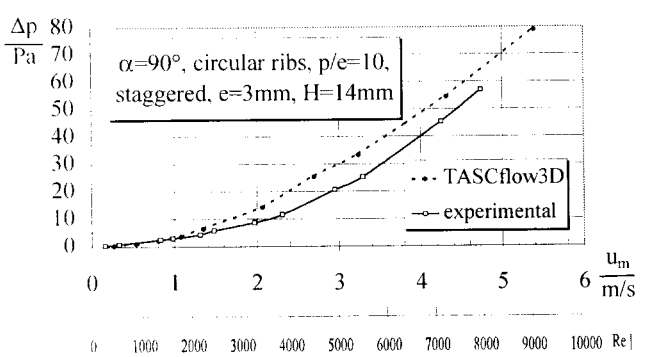

Figure 12. Pressure drop
(numerical calculations and experimental results)

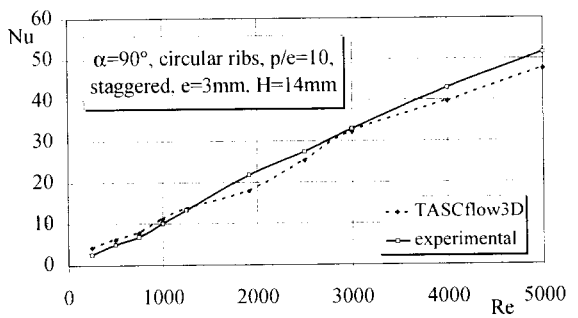

Figure 13. Mean Nusselt number
(numerical calculations and experimental results)

6. NOMENCLATURE

A	total heat transfer area, m^2
A_c	flow cross-sectional area, m^2
b	rib width at base, m
d_{hyd}	hydraulic diameter $d_{hyd} = 4\ A_c/U$, m
e	rib height, m
H	height of duct, m
h	heat transfer coefficient, $W\ m^{-2}K^{-1}$
k	fluid thermal conductivity, $W\ m^{-1}\ K^{-1}$
L	length of duct, m
Nu	Nusselt number
	$Nu = h\ d_{hyd} / k$, dimensionless
p	rib spacing, m
p	pressure, Pa
$\dot{Q}$	heat transfer rate, W
Re	Reynolds number
	$Re = \rho\ w\ d_{hyd} / \mu$, dimensionless
T	temperature, °C, K
Tu	turbulence intensity
	$Tu = [0.5(u'^2+v'^2)]^{1/2} / u_m$,dimensionless
U	flow cross sectional perimeter, m
u,v,w	velocity components, $m\ s^{-1}$
u´,v´,w´	turbulent fluctuation velocity components, $m\ s^{-1}$
W	width of duct, $m\ s^{-1}$
w_m	fluid mean velocity, $m\ s^{-1}$
x,y,z	coordinates in channel, m
α	rib angle of inclination vs. main flow direction, °
λ	laser beam wavelength. nm
μ	fluid dynamic viscosity, Pa s
ξ	friction factor, dimensionless
ρ	fluid density, $kg\ m^{-3}$
φ	circular segment angle, °

7. REFERENCES

Bergles, A.E., 1995, Heat Transfer Enhancement - The Encouragement and Accomodation of High Heat Fluxes, Max Jakob Memorial Award Lecture, *Journal of Heat Transfer*

Bergles, A.E., Jensen, M.K., Shome, B., 1995, Bibliography on Enhancement of Convective Heat and Mass Transfer, *Heat Transfer Laboratory Report HTL-23*

Bergles, A.E., 1996, The Encouragement and Accommodation of High Heat Fluxes, *Proc. of the 2nd European Thermal Science Conference*, pp.3-11, Rome,

Fiebig, M., 1996, Vortices: Tools to Influence Heat Transfer-Recent Developments, *Proc. of the 2nd European Thermal Science Conference*, pp. 41-56, Rome

Gröber, Erk, Grigull, **U.**, 1955, Die Grundgesetze der Wärmeübertragung, Springer-Verlag, Berlin

Han, J.C., Heat Transfer and Friction in Channels with Two Opposite Rib-Roughened Walls, *Transactions of the ASME*, pp. 774-781. Vol. 106, November 1984

Hauf, W., Grigull, U.. 1970, Optical Methods in Heat Transfer, *Advances in Heat Transfer*, Vol. 6, Academic Press, New York

Kreipe, E., 1985, Wärmeübergang und Strömungswiderstand in Rohren mit künstlichen Rauhigkeiten, *Dissertation*, University of Hannover

Mayinger, F., Chen, Y.M.. 1985, Holographic inter-ferometry studies of the temperature field near a condensing bubble, Optical methods in dynamics of fluids and solids, *Proc. of an int. Symposium IUTAM*, Berlin

Mayinger, F., Panknin, 1974, W., Holography in Heat and Mass Transfer, *Proc. of the 5th Int. Heat Transfer Conference*, Tokyo

Mayinger, F., Klas, J., 1993, Investigation of Local Heat Transfer in Compact Heat Exchangers by Holographic Interferometry, *Proc. of the First International Conf. on Aerospace Heat Exchanger Technology*, pp. 449-465, Palo Alto

Rifert, V.G., Shavrin, Yu.V., et al., 1996, Investigation of Forced Convectional Heat Exchange in Flat-Oval Channels with Profiled Surface, *Proc. of the 2nd European Thermal Science Conference*, pp. 631-634, Rome

Zukauskas, A., 1989, *High-Performance Single Phase Heat Exchangers*, Hemisphere Publishing Corporation, New York